THIS PAPER WAS PRESENTED AT THE SYMPOSIUM ON JULY 11 2003
TO CELEBRATE THE LIFETIME CONTRIBUTIONS OF
PROFESSORS EMERITI TOM PAULAY AND BOB PARK

DOES CAPACITY DESIGN DO THE JOB? AN EXAMINATION OF HIGHER MODE EFFECTS IN CANTILEVER WALLS

M.J.N. Priestley[1]

ABSTRACT

Current provisions in the New Zealand Loadings code for dynamic amplification of moment and shear force in cantilever wall buildings are critically examined. Based on time-history analyses of six wall structures, from two- to twenty-storeys, it is found that higher mode effects are inadequately represented by either the equivalent lateral force or modal response spectrum design methods. The time-history results indicate that dynamic amplification is dependent on both initial period, and expected displacement ductility level.

Two different methods for consideration of higher mode effects in cantilever walls are proposed. The first is based on a simple modification of the modal response spectrum method, while the second is appropriate for single-mode design approaches such as the equivalent lateral force method. Both are found to give excellent representation of expected response. It is shown that providing capacity protection at the design seismic intensity does not ensure against undesirable failure modes at intensities higher than the design level. This has significance for the design of critical facilities, such as hospitals.

BIOGRAPHICAL NOTE

Nigel Priestley is an Emeritus Professor of Structural Engineering at the University of California, San Diego, and is co-director of the European School for Advanced Studies in the Reduction of Seismic Risk (the "Rose School") at Pavia, Italy. He obtained his Batchelor's and Doctoral degrees from Canterbury University, having been one of Tom Paulay's "victims" as an undergraduate, with Bob Park supervising the final stages of his PhD. After ten years in the wilderness of the Ministry of Works Central Laboratories, he returned to the University of Canterbury fold, where for ten years he worked closely with both Tom and Bob on various seismic research topics. He has published many research documents with either (and in some cases both) Tom and Bob, including a book with Tom that has been a source of mystery and confusion to many students and professionals over the past ten years. Primarily this is a result of the inadequate fulfillment of Nigel's major role in the book, which was to translate Tom's Hungarian into English.

In the mid 1980's Nigel escaped from Canterbury to the United States, and more latterly to Italy, during which time he has attempted to convince anyone who would listen that almost everything we do in earthquake engineering is wrong. He occasionally dons false nose and moustache and sneaks back, unobserved, he hopes, into New Zealand.

---

[1] *Co-director, European School for Advanced Studies in the Reduction of Seismic Risk (the "Rose School") at Pavia, Italy, (Fellow).*

1. INTRODUCTION

A fundamental requirement of New Zealand seismic design is the incorporation of capacity design considerations. Based largely on work by Paulay and Park (Park and Paulay, 1976), New Zealand was the first country to incorporate detailed and specific capacity design requirements in design codes. Indeed, though some other codes, notably the Eurocode EC8 (CEN, 1998) have recently incorporated capacity design provisions, others, particularly those in the United States, still have only rudimentary capacity design rules.

Capacity design is the process by which relative strengths of different members and actions are chosen to ensure that only the designer's intended inelastic mechanism can be developed in a structure during strong seismic attack. Thus columns are allocated higher relative strengths than beams in a frame design, to ensure the desired weak-beam/strong-column mechanism develops, and shear strengths are uniformly enhanced over flexural strengths to ensure that inelastic deformation occurs only in a flexural mode. The procedure is intended to "desensitize" the structure to earthquake characteristics – particularly to the frequency content (including the temporal distribution thereof), and to a lesser extent, to the magnitude: it is recognized that an earthquake with higher local intensity than the design level will probably induce increased ductility demand, but the capacity design process should protect against undesirable deformation modes, even for larger-than-design intensity.

The basis for capacity design in New Zealand (NZS4203,1992) is that required flexural strength at intended potential plastic hinges is determined from one of three different analysis techniques: equivalent lateral force; modal superposition, or time-history analysis. Required strengths at other locations, or due to other actions than flexure (such as shear), are found by capacity design considerations. Basic strengths for these locations and actions corresponding to the initial analysis are amplified by an overstrength factor ϕ^o to account for potential flexural overcapacity at the plastic hinge locations resulting from excess reinforcement and/or higher than anticipated material strengths (including strain-hardening, and concrete confinement), and also by a dynamic amplification factor ω to represent the potential increase in design actions due to higher mode effects. The required strength is thus:

$$S_R = \phi^o \omega S_E \qquad (1)$$

where S_E is the value of the action considered, based on the initial analysis, and S_R is the required strength, based on capacity considerations.

The values for ϕ^o and ω to be considered in design depend on the initial method of analysis, the action being considered (e.g. flexure, or shear), and the structural form (e.g. structural wall or frame). If design actions are based on inelastic time-history analysis (**THA**), dynamic amplification is explicitly considered, and flexural overstrength can also be directly considered by a second analysis, using overstrength material properties, and moment-curvature relationships that include strain-hardening and confinement. In this case, no modification of the analysis results is needed to satisfy capacity design requirements.

At the other end of the scale of analysis techniques is the equivalent lateral force (**ELF**), where required strengths at potential plastic hinges is determined from a simplified representation of the first mode inelastic force distribution. Typically, and conservatively, 100% of the mass is considered to act in the first mode. The first-mode period is often estimated from extremely conservative height-dependent equations (e.g. CEN-1998, IBC, 2000), but in New Zealand (NZS4203, 1992), is estimated from the Rayleigh equation, using realistic estimates of member stiffness.

For the required moment capacity of cantilever walls, the base moment is amplified to account for material overstrength, and a linear distribution of moments is generally adopted up the wall height to account for higher mode effects. As is apparent from Figure 1(a), this implies higher amplification of moments at midheight than at the base or top of the wall. Reinforcement cut-off is determined by consideration of tension shift effects. This is achieved by vertical offset of the moment profile. The design moments thus do not exactly follow the form of Eq. (1). In New Zealand design, an additional portion of the lateral base shear force is required to be applied at roof level at roof level. This is not shown in Fig.1.

Shear forces corresponding to the Equivalent Lateral Force distribution are amplified by the flexural overstrength factor, and the dynamic amplification factor ω_v directly in accordance with Eq. (1), as shown in Fig. 1(b). The form of the dynamic amplification factor, given in Eq. (2), depends only on the number of storeys of the building (NZS3101,1995).

$$\begin{aligned} \omega_V &= 0.9 + n/10 \qquad for \quad n \le 6 \\ \omega_V &= 1.3 + n/30 \qquad for \quad 6 < n < 15 \end{aligned} \qquad (2)$$

where n is the number of stories in the wall, and need not be taken greater than 15. An additional limitation is placed that the shear force should not exceed μV_E, where V_E is the shear force resulting from the initial analysis, and μ is the design displacement ductility level. Thus, Eq. 1 may be rewritten:

$$V_R = \phi^o \omega_v V_E \le \mu V_E \qquad (3)$$

For frame structures, beam shear forces, and moments at locations other than potential plastic hinges are amplified by the flexural overstrength factor. Since higher modes, including vertical seismic response, are not normally considered for beam design, the dynamic amplification factor is not normally included.

Column end moments and shear forces are amplified for both beam plastic hinge overstrength and dynamic amplification. For one-way frames, upper limits for the dynamic amplification of column moments of 1.80 have been recommended, with 1.3 for column shear forces. Further amplification for beam flexural overstrength is required.

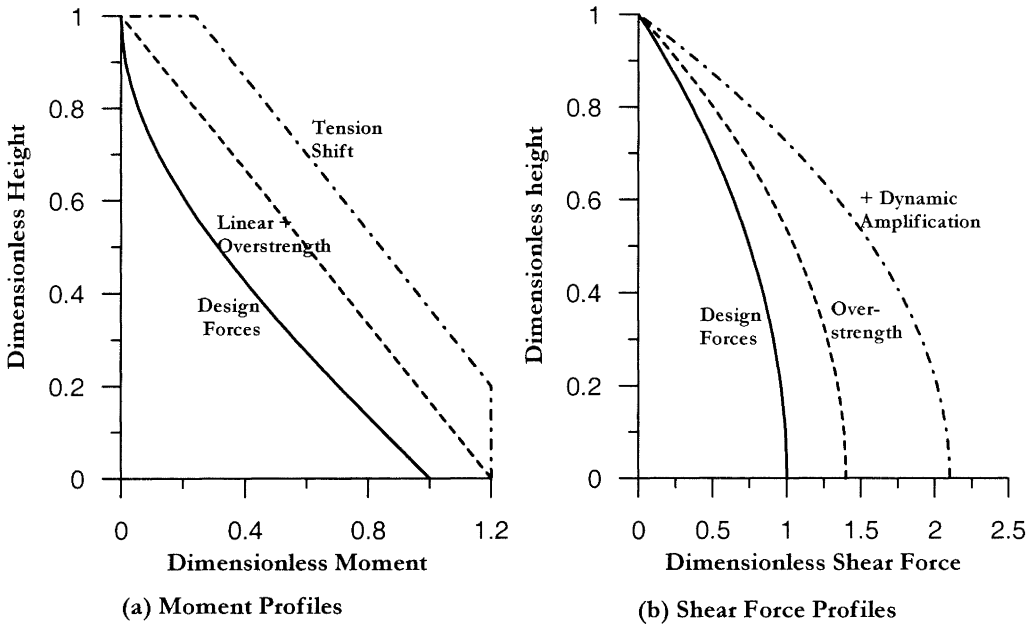

Figure 1. Dynamic Amplification of Design Forces for Equivalent Lateral Force Design Of Cantilever Walls.

When modal response spectral analysis (**MRS**) forms the basis of seismic design, the higher mode effects are directly considered in the analysis, since all significant elastic modes, rather than just the fundamental mode, are included when determining the design forces. The individual response of each significant mode, in terms of lateral forces, element bending moments or shear forces, and displacements are found from direct modal combination of the relevant action or displacement. Adopting the SRSS combination for simplicity, the elastic forces and displacements are thus given by:

$$F_{ie} = \sqrt{\sum_{i,m=1}^{N} F_{im}^2}\ ,\quad M_{ie} = \sqrt{\sum_{i,m=1}^{N} M_{im}^2}\ ,$$

$$V_{ie} = \sqrt{\sum_{i,m=1}^{N} V_{im}^2}\ ,\quad \text{and}\quad \Delta_{ie} = \sqrt{\sum_{i,m=1}^{N} \Delta_{im}^2} \qquad (4)$$

where N is the number of significant modes considered. In most seismic design codes, M_{im} and V_{im} are the moments and shears induced by the elastic modal forces F_{im} calculated from the elastic response spectrum. The design forces are then determined by dividing the elastic forces by the behaviour (force-reduction) factor, R, and the design displacements are taken as equal to the elastic displacements. Thus:

$$F_{iD} = \frac{F_{ie}}{R},\quad M_{iD} = \frac{M_{ie}}{R},\quad V_{iD} = \frac{V_{ie}}{R},$$

$$\text{and}\ \Delta_{iD} = \Delta_{ie} \qquad (5)$$

In the NZ Loadings Code (NZS4203, 1992), an inelastic spectrum, related to the period of the first elastic translational mode by a factor S_m and the structural ductility factor μ is used to calculate the forces, moments and shears in Eq. (4), and hence no further modification for force-reduction is required in Eq. (5). The displacements from Eq. (4) are then increased by the displacement ductility factor to provide the expected design response displacements.

The assumption inherent in the above formulations is that the behaviour factor R, or the displacement ductility factor μ applies equally to all modes. A corollary of this is that design forces of a designed structure are unaffected by the seismic intensity, provided that the intensity is sufficient to induce inelastic response. This is because (say) doubling the seismic intensity will be equivalent to doubling the behaviour factor. Although the elastic response forces, moments and shears will all double, the strengths of the plastic hinges will remain as designed, and hence the effective behaviour factor for the increased intensity must increase proportionately. Since the increased behaviour factor applies to all modes, the design forces, given by Eq. (5) are unchanged. Since the displacements are equal to the elastic displacements, however, the displacement response (and hence the displacement ductility demand) will be increased in direct proportion to the increase in seismic intensity.

It is not clear from the New Zealand Loadings code whether dynamic amplification factors are to be applied to structures whose design forces have been determined from modal analysis. However, since the forces directly consider the higher mode effects, it would be reasonable to assume that no further dynamic amplification would be needed. It is also worth noting that the Loadings code does not require specific dynamic amplification when the design displacement ductility level is less than 3.

2. HIGHER MODE EFFECTS IN CANTILEVER WALLS FROM TIME-HISTORY ANALYSIS

2.1 Wall Designs

The dynamic amplification factors of Eq. (2) are based on inelastic time-history analyses carried out in the mid-1970's

(Blakeley *et al*, 1975). These analyses used values for wall stiffnesses, and hysteretic rules that would no longer be considered appropriate for realistic modelling of dynamic response. In order to investigate the significance of the earlier assumptions, and to provide new information on dynamic amplification factors, an analytical research project was recently carried out (Priestley and Amaris, 2002). Six walls, from 2 storeys to 20 stories were designed to the Eurocode EC8 elastic acceleration response spectrum of Fig. 2, which is compatible with a peak ground acceleration of 0.4g, and a medium soil condition (subsoil class B, characterized by deep deposits of medium dense sand, gravel, or medium stiff clays). For comparative purposes, Fig. 2 also includes the elastic acceleration design spectra according to NZS4203 for an intermediate soil, and a zone factor of Z=1.2, with and without the performance factor $S_p = 0.67$. It will be seen that when the S_p is included, the NZS4203 design spectrum for the most active seismic regions of New Zealand is 33% lower than the EC8 spectrum for 0.4g PGA, but excluding the performance factor (the S_p factor is particularly hard to justify for cantilever wall buildings) the spectra are identical for periods above 1.0 seconds. The low maximum intensity NZ design spectrum compared with European practice may be surprising to some.

The walls (see Fig. 3) all had the same tributary floor mass of 60 tonnes, and gravity load of 200 kN at each level, and were designed in accordance with direct-displacement based design principles (Priestley, 2000) to achieve maximum drifts (interstorey displacement divided by interstorey height) of approximately 0.02 at the critical top storey, under the design levels of seismic intensity. Wall lengths (l_w), widths (b), reinforcement contents (ρ_l) and bar sizes (d_b) varied from wall to wall in order to satisfy the design displacement criteria. Details are listed in Table 1, which also includes the calculated plastic hinge

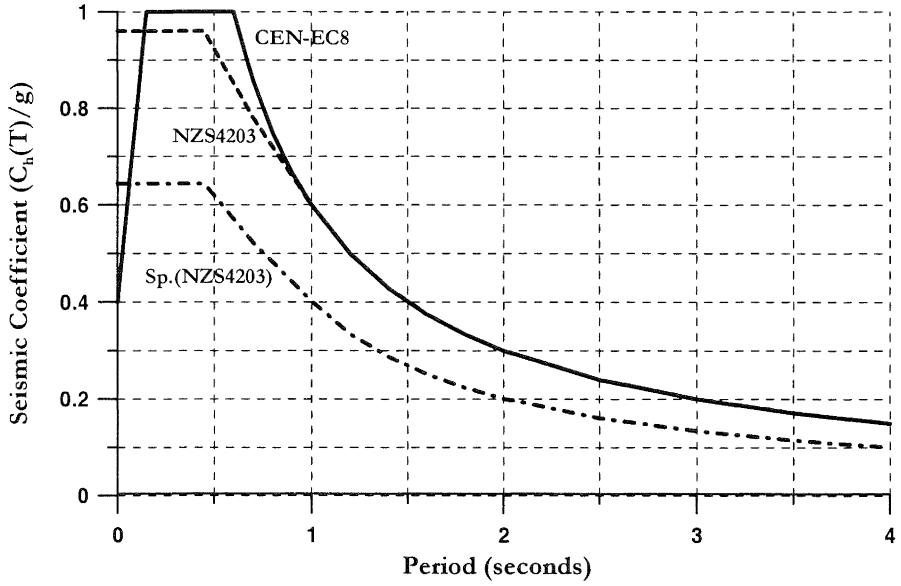

Figure 2. Comparison of EC8 spectrum for 0.4g PGA with NZS4203 for Z = 1.2

length (l_p), the expected displacement and curvature ductility demands (μ_Δ, μ_ϕ), the effective period at maximum displacement (T_{eff}, approximately equal to $T_{el}\cdot\sqrt{\mu_\Delta}$), and design base shear force and bending moment (V_b, and M_b). Note that limiting the drift to 0.02 results in displacement ductility levels that are less than the code limit of 5 in all but the two-storey wall.

Again for comparative purposes, in addition to designing the walls with direct-displacement based design principles, the walls were also designed to NZS4203 requirements, using the Equivalent Lateral Force (**ELF**) approach, and modal response spectral analysis (**MRS**). For these designs, elastic stiffnesses calculated for the displacement-based designs were assumed to apply directly. All walls were designed assuming a displacement ductility factor of 5.0, as permitted by the NZ Concrete Code (NZS3101, 1995).

Distributions of moments and shears corresponding to the calculated lateral force distributions from the three design approaches are compared in Figs. 4 and 5 respectively. These do not include any dynamic amplification for higher mode effects. Modal response spectral analysis results are indicated by **SRSS** (the square-root-sum-of-squares combination rule was used as the modes were well separated). Equivalent lateral force, and displacement-based design results are indicated by **ELF** and **DBD,** respectively. Also included in the figures is a fourth set of design profiles, denoted **SSRS/**μ. These profiles amplify the design forces of the modal spectral analyses by the amount to provide the identical design base moment as for the displacement-based designs. This facilitates comparison of the influence of higher modes in the modal response spectral analysis approach, and represents designs, which should satisfy the code drift limits.

From the moment profiles of Figure 4, it is apparent that design to NZS4203 results in significantly reduced design base moments compared to those resulting from displacement based design. The implication is that under seismic intensity represented by the EC8 elastic acceleration spectrum, the NZ designs, both **ELF** and **MRS** would be expected to develop peak drifts in excess of the code limit of 0.02, which was used for the displacement-based designs. It should be noted that the reduced design spectrum represented by the S_p.NZS4203 curve in Fig. 2 is not a measure of the

design intensity, but of required strength to satisfy displacement demands of the full spectrum. Checking of expected displacements would reveal the excessive drifts, and redesign to higher lateral forces would be required. Note that these results would appear to indicate that the ductility limit of $\mu = 5$ will almost always result in excessive drifts.

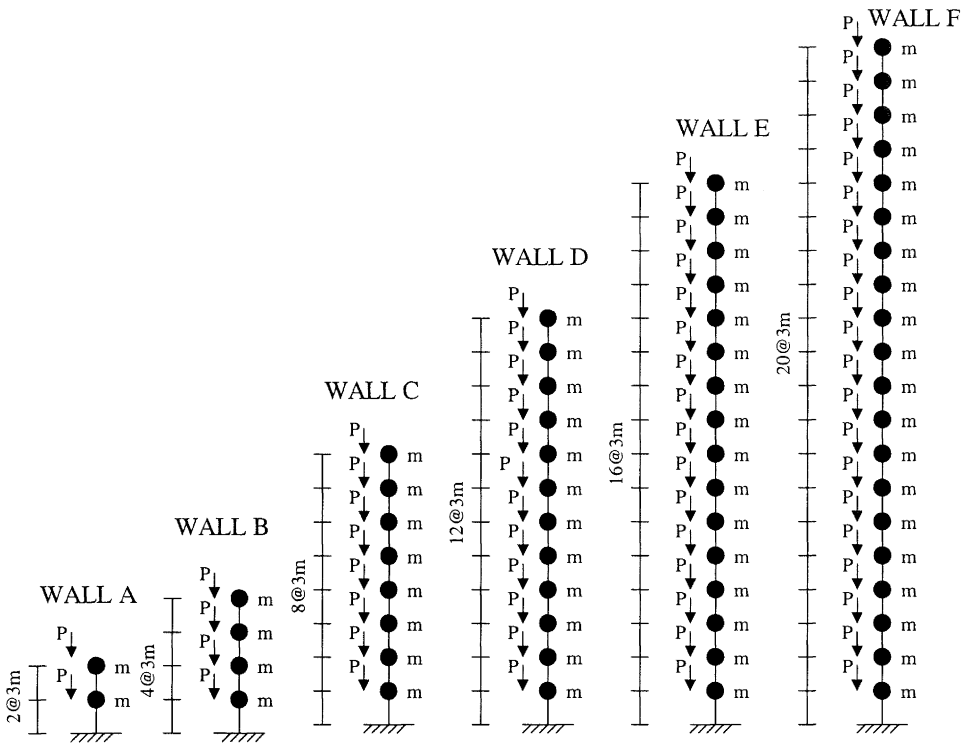

Figure 3. Idealization of Cantilever Walls

Table 1. Wall Details for Cantilever Wall Study

Wall	b (m)	l_w (m)	ρ_l	d_b (mm)	l_p (m)	μ_Δ	μ_ϕ	T_{eff} (sec)	V_b (kN)	M_b (kNm)
A	0.20	2.0	0.0046	14	0.58	6.4	20.6	1.2	242	1232
B	0.20	2.5	0.0080	14	0.86	3.4	12.6	1.8	312	2917
C	0.20	3.3	0.0162	20	1.49	1.9	6.0	2.6	446	8114
D	0.25	4.0	0.0172	28	2.22	1.3	2.7	3.1	590	16222
E	0.25	5.0	0.0161	24	2.83	1.2	2.2	3.7	664	24372
F	0.30	5.6	0.0177	28	3.52	1.0	1.0	3.9	830	38739

The **SRSS** and **ELF** results in Figure 4 do not consider the minimum seismic coefficient of 0.03 required by NZS4203. This is discussed further in relation to Figure 5. It will be noted that the **ELF** approach always results in base moments substantially higher than the SRSS values, with the difference often being greater than 20%. When the **SSRS** values are scaled up to the same base moment as the **DBD** results, the effects of higher mode response are clearly visible, particularly for the eight- to twenty-storey walls.

Shear force distributions in Figure 5 show similar trends, though there are also significant differences. It is seen that except for the two- and four-storey walls, base shear from the **SSRS** exceeds that from the **ELF**. In all cases the **SSRS** base shears exceed 80% of the **ELF** results, and hence, according to NZS4203, no scaling up of the design forces is required. Note that despite this, the base moments, which have greater influence on the displacement and drift demand, are always smaller than the **ELF** results, and frequently by more than 20%, as noted above. Scaling up the SSRS forces to provide the same base moment as the **DBD** designs (and hence, presumably satisfying the code drift limits), results in shear force profiles that exceed the **DBD** shear force profiles by an amount that increases with the number of storeys. For the sixteen- and twenty-storey walls, the SSRS/μ base shears

are more than twice the **DBD** results, indicating dynamic amplification higher than specified by Eq. (2). The influence of higher modes is also clearly apparent in the "bulges" of shear force near the top of the twelve- to sixteen-storey walls.

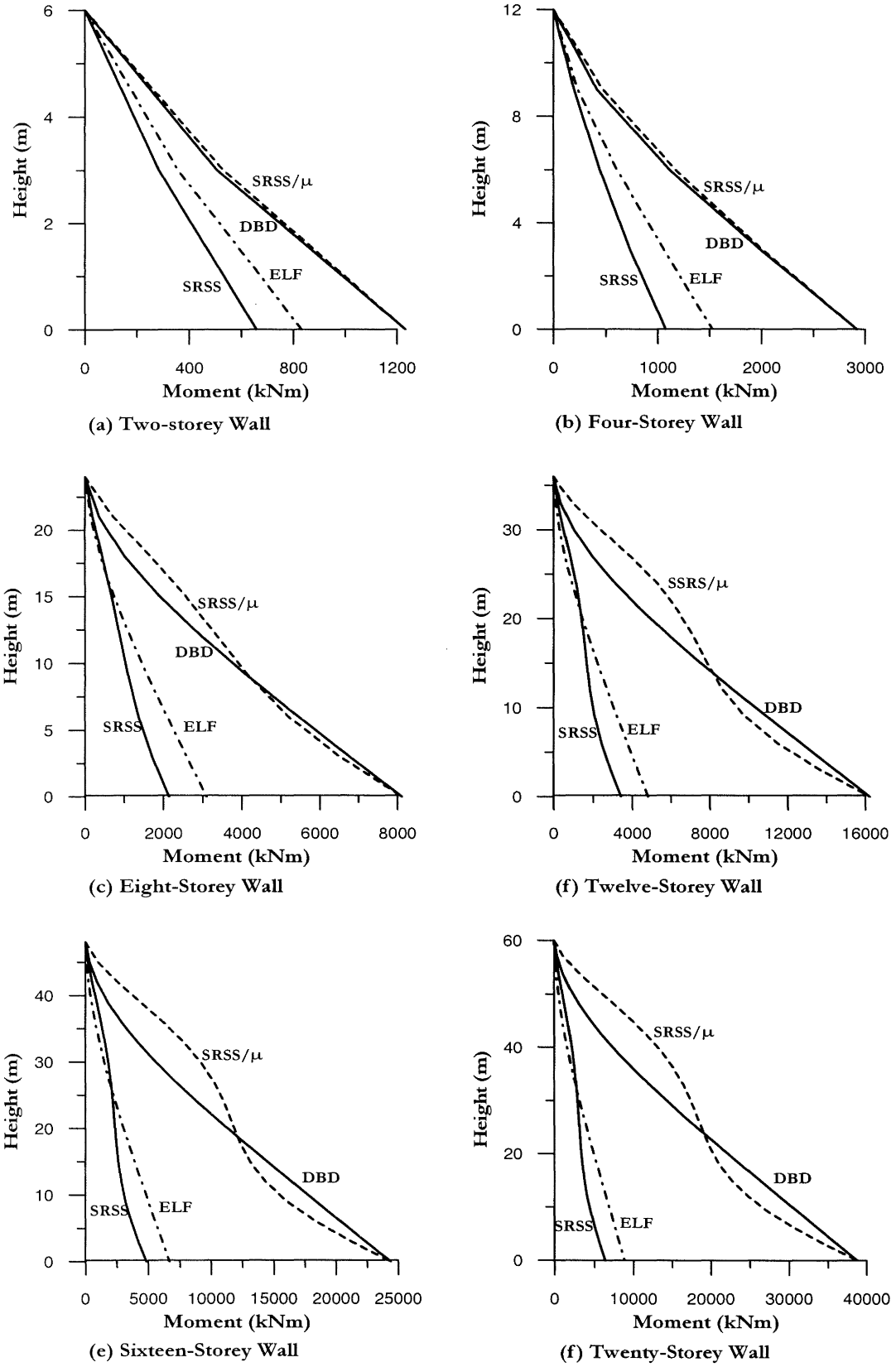

Figure 4. Wall Design Moment Profiles to Spectra of Figure 2 from Different Design Procedures.

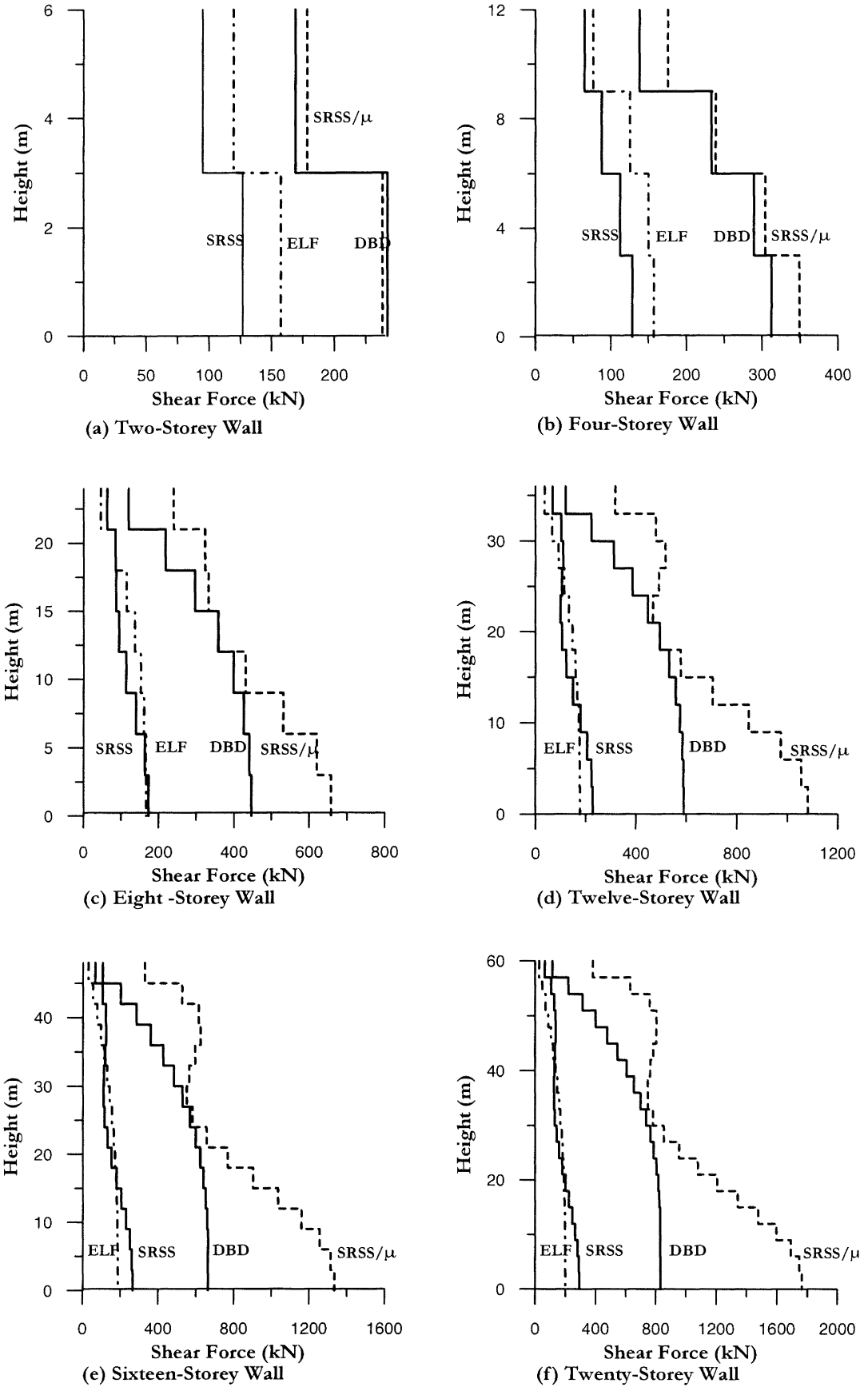

Figure 5. Wall Design Shear Force Profiles to Spectra of Figure 2 from Different Design Procedures.

The NZS4203 minimum seismic coefficient of 0.03 has not been applied to the shear force distributions of Figure 6. In fact, the SSRS distributions of the 16 and 20 storey walls result in base shear forces that are lower than the 0.03 limit by 6% and 17% respectively. Base shears for the **ELF** approach are less than the 0.03 limit for 12, 16 and 20 storey walls, by 18%, 35% and 44% respectively. Making the appropriate adjustments would not change any of the above conclusions.

2.2 Results of Time-History Analyses

The six displacement-based wall designs were subjected to time-history analyses using a suite of five artificial earthquake records compatible with the EC8 spectral shape of Fig. 2. These records were intensity scaled to investigate the influence of intensity ratio on moment and shear force envelopes. The computer code *Ruaumoko* (Carr, 1998) was used for the analyses, with hysteretic behaviour of potential plastic hinge regions represented by a realistic modified Takeda hysteresis rule. Note that higher mode effects are rather sensitive to the hysteretic model assumed, and earlier work (Blakeley *et al*, 1975) was carried out on the less realistic simplified elasto-plastic hysteresis rule.

Moment and shear force envelopes from the time-history analyses at different seismic intensities are compared with the **SRSS/□** and capacity design values in Figs. 6 and 7 respectively. In these figures, "IR" indicates "intensity ratio", or the multiple of the design seismic intensity. Thus "IR = 1" indicates the design intensity, "IR = 0.5" indicates 50% of design intensity, and so on. The capacity design values for moment and shear, indicated by dash-dot lines with the label **Cap.Des** to the left of the line, include only the dynamic amplification, since material overstrength was not included in the analyses. Thus, for moment profiles the capacity design curve is a straight line from the base moment to zero at the wall top. Note, however, that the wall base moments from time history exceed the capacity design base moment by small amounts due to strain-hardening. Capacity design shear forces are the **DBD** values amplified in accordance with Eq.(3), with $\phi^o = 1.0$. The **SRSS/μ** values, indicated by dashed lines with the label **SSRS/μ** to the left of the line are identical to those in Figs. 4 and 5, on the basis that **MRA** provides explicit representation of higher mode effects.

Referring first to Figure 6, we see that the time-history analysis results indicate only small increases in base bending moment with increasing intensity, as expected, since the increase, once the nominal moment capacity has been reached is only the result of the post-yield stiffness of the moment-curvature characteristic at the wall base. However, at levels above the base, and particularly at wall mid-height, moments increase very significantly with increasing intensity, especially for the eight- to twenty-storey walls. Note that as multi-modal analysis is currently formulated, in accordance with Eq. (4) and (5), the only increase in moments with increasing intensity would be in proportion to the strain-hardening increase at the wall base. It is also apparent that the multi-modal analysis (**SRSS/μ**), is non-conservative at the design intensity, (IR = 1.0) and increasingly so at higher intensities. For the two- to eight-storey walls, where the design displacement ductilities exceed 2 (see Table 3.1), the multi-modal moment envelope is non-conservative even at 50% of the design intensity.

Similar conclusions apply to the linear capacity design envelope, which is consistently non-conservative for intensities at or higher than the design intensity. It is only conservative for IR = 0.5 when the design level of displacement ductility is less than $\mu = 2.0$.

In Figure 7 it is again seen that the time-history shear force envelopes are strongly influenced by seismic intensity, (and hence by ductility level), and that both the capacity design and multi-modal design envelope are significantly non-conservative. For the two-, four- and eight-storey walls, the time-history base shear force at IR = 1 is almost twice the multi-modal value, with a slightly smaller discrepancy for the capacity design envelope, and for these three walls, the shear profiles at IR = 0.5 exceed the design profile at all heights. At intensity ratios of IR = 2, base shear force is between 2.5 and 3.7 times the multi-modal design envelope. For the taller walls the **SSRS/μ** envelope exceeds the capacity design envelope, and thus the discrepancy from the capacity design value is even higher.

The discrepancies between the capacity design and time-history shear forces are more problematic than the corresponding moment discrepancies of Figure 6. Although unintentional plastic hinging (which could be the consequence of designing to either the **MMS** or **SSRS/μ** capacity moment envelopes of Fig. 6) at levels above the base is undesirable, some limited ductility demand should be sustainable without failure. However, the consequences of the imposed shear demand exceeding the shear capacity, by such large margins, could be catastrophic shear failure.

2.3 Modified Modal Superposition for Design Forces in Cantilever Walls

Examination of Figure 7 indicates that at an intensity ratio of IR = 0.5, where ductility demand is low, or non-existent for all walls, the shape of the shear force envelope is well predicted by the modal analysis procedure. This suggests that it might be possible to predict the shear force and moment envelopes by simple modification of the modal response spectrum (**MRA**) approach.

A basic and simple modification to the modal superposition method is available by recognizing that ductility primarily acts to limit first mode response, but has comparatively little effect in modifying the response in higher modes. If this were to in fact be the case, then first mode response would be independent of intensity, provided that the intensity was sufficient to develop the base moment capacity, while higher modes would be directly proportional to intensity. This approach is very similar to that proposed by Eibl and Keintzel (Eibl and Keintzel, 1988) as a means for predicting shear demand at the base of cantilever walls.

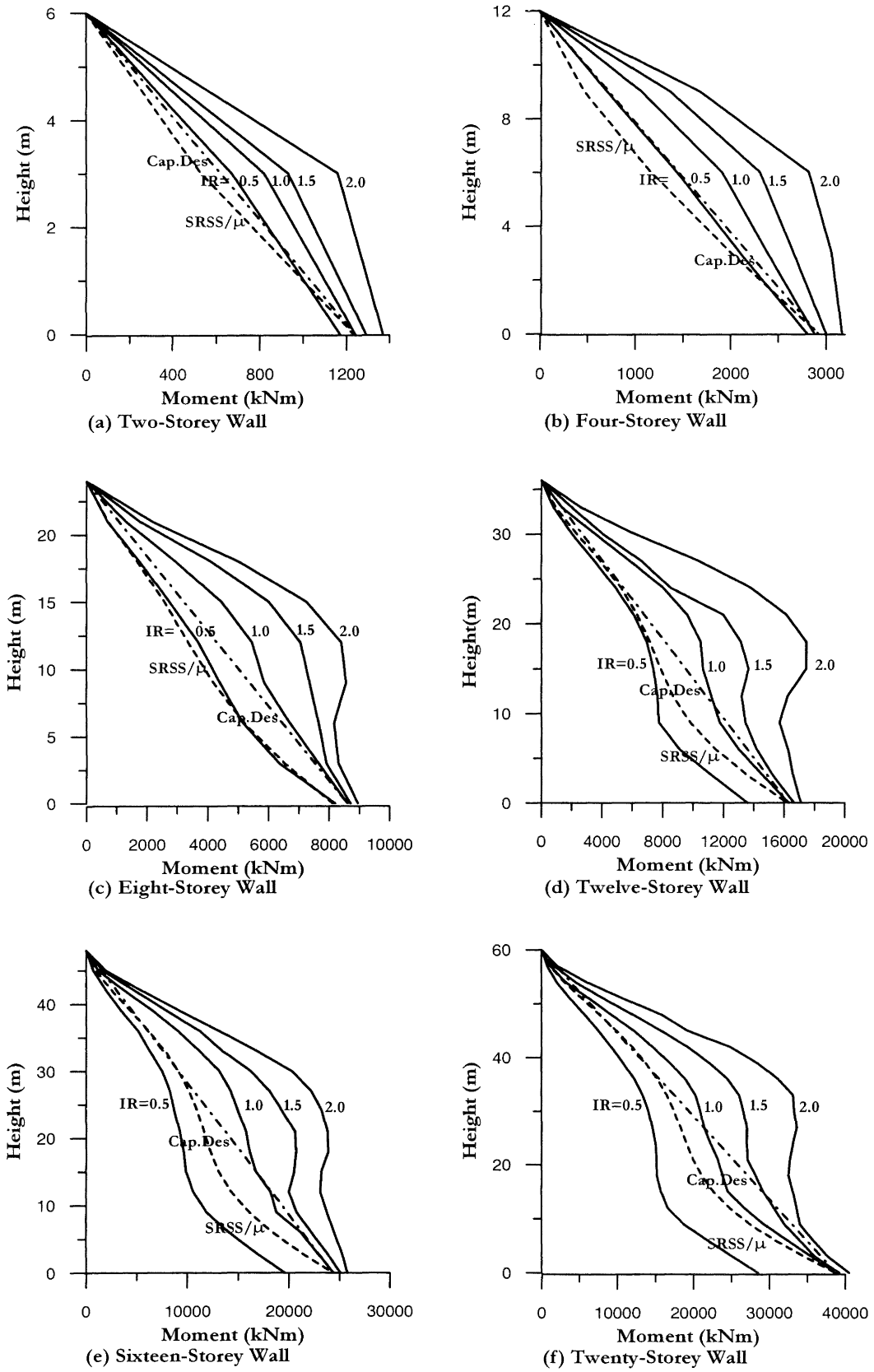

Figure 6. Comparison of Capacity Design Moment Envelopes with Results of Time-History Analyses For Different Seismic Intensity Ratios.

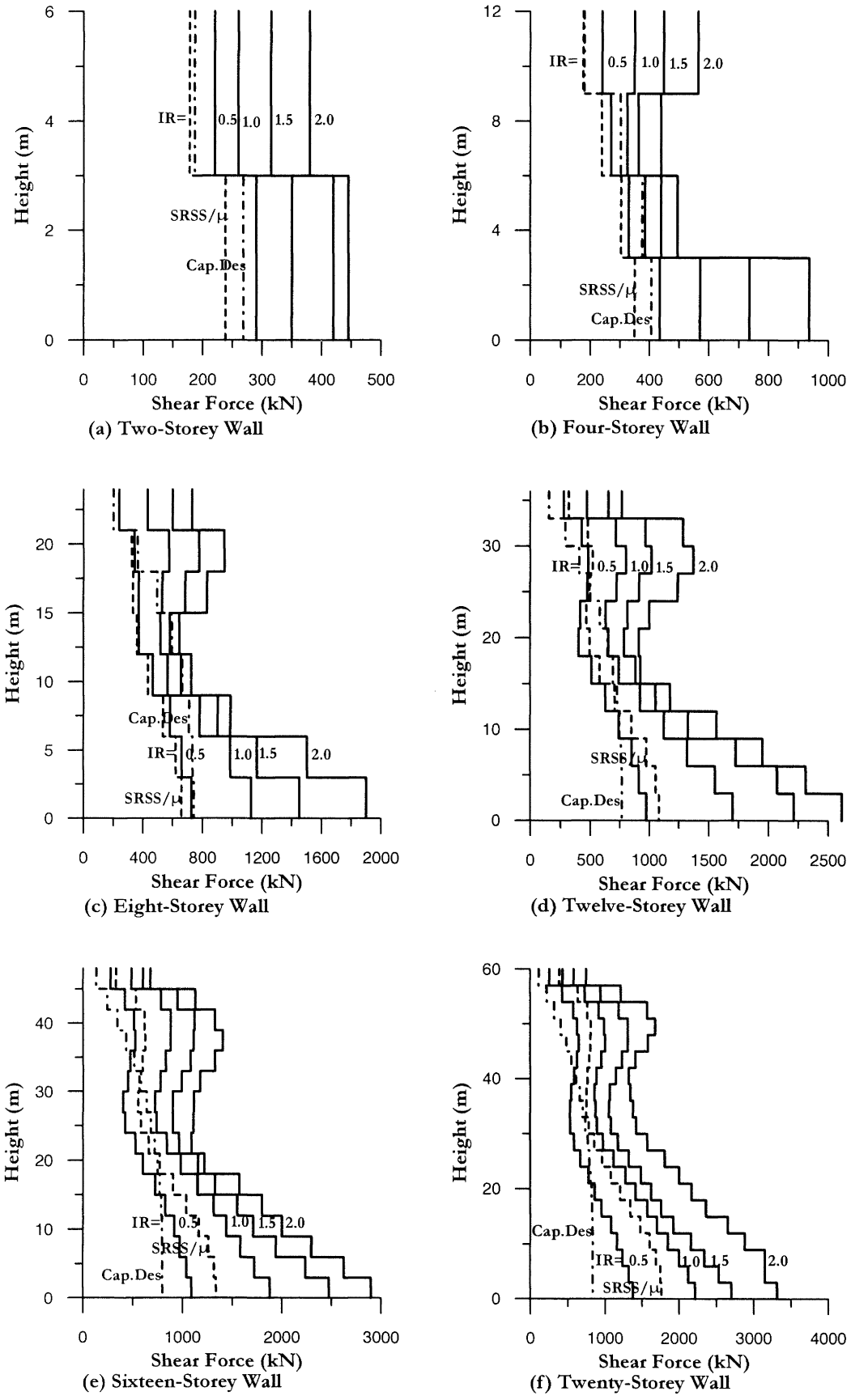

Figure 7. Comparison of Capacity Design Shear Force Envelopes with Results of Time-History Analyses for Different Seismic Intensity Ratios.

This modified modal superposition approach is clearly an approximation to response. Although the first mode inelastic shape is very similar to the elastic shape, and hence the approximation should be reasonably valid for the first mode, it is clear that the higher modes will be modified to some extent by the first mode ductility, since a basic feature of the modified higher modes will be that, when acting together with ductility in the first mode, they cannot increase the base moment demand, which will be anchored by the moment capacity of the base plastic hinge. The approach suggested below attempts to extend the basic method of Eibl and Kreintzel for shear forces to the full height of the wall, and also to provide a method for determining the appropriate capacity design moment envelope.

Shear Force Profiles: To investigate the appropriateness of a simple approach based on the above arguments, shear force profiles were calculated based on the following assumptions.

- First mode shear force was equal to the shear profile corresponding to development of the base moment capacity, using the displacement-based design force vector. However, for low seismic intensity, where plastic hinging was not anticipated in the wall, simple elastic first mode response, in accordance with the elastic response spectrum was assumed.
- Higher mode response was based on elastic response to the acceleration spectrum appropriate to the level of seismic intensity assumed. Force-reduction factors were not applied.
- The basic equation to determine the shear profile was thus:

$$V_i = (V_{1i}^2 + V_{2Ei}^2 + V_{3Ei}^2 + ...)^{0.5} \quad (6)$$

where V_i is the shear at level i, V_{1i} is the lesser of elastic first mode, or ductile first mode response at level i, and V_{2Ei}, and V_{3Ei} etc are the elastic modal shears at level i for modes 2, 3 etc. Predictions for shear force profiles based on this equation are included in Figure 9.

Moment Profiles: It is clear that the simple modal combination used for shear forces cannot be directly used for moments. This is because such an approach would predict increasing base moment with increasing intensity ratio, whereas the base moment is anchored to the capacity of the wall. As a consequence, the higher mode moment patterns are likely to deviate significantly from the elastic mode shapes, particularly in the lower regions of the wall.

A simple modal combination, similar to that of Eq. (6), but multiplied by a factor of 1.1, over the top half of the wall, with a linear profile from mid-height to the moment capacity at the base of the wall was found to provide best results (see Fig.8). The combination equation over the top half of the wall is thus:

$$M_i = 1.1 \times (M_{1i}^2 + M_{2Ei}^2 + M_{3Ei}^2 + ...)^{0.5} \quad (7)$$

where M_i is the moment at level i, M_{1i} is the lesser of the elastic first mode moment and the ductile design moment, and M_{2Ei} and M_{3Ei} etc are the elastic modal moments at level i for modes 2, 3, etc.

Comparison with Time-history Results: The predictions of this Modified Modal Superposition (**MMS**) approach are compared in Figs. 8 and 9 with time-history results for moment profiles and shear force profiles respectively for the six different wall heights, at the different levels of seismic intensity. Average results from the time-history analyses are indicated by solid lines, with the **MMS** predictions indicated by dashed lines.

It is seen that the **MMS** approach provides a good representation of the time-history moment profiles in Fig. 8 at the design intensity (IR = 1.0), for all walls. There is a tendency for the **MMS** predictions to be slightly unconservative for the shorter walls, and slightly conservative for the taller walls, though the discrepancies are generally small. The change in shape of the moment profiles with increasing intensity is also well represented by the **MMS** predictions, though trends apparent at IR = 1.0 are accentuated at higher intensities.

Similar behaviour is apparent for the shear force comparisons of Figure 9. At the design intensity the agreement between the **MMS** and **THA** profiles is extremely close for the four- to twenty-storey walls, and is adequate, though a little unconservative for the two-storey wall. Similar conclusions apply at different intensity levels, though the **MMS** approach becomes increasingly conservative for the taller walls at high intensity ratios.

2.4 Consequences for Capacity Design

It is clear from the results presented in Figures 6 and 7 that current capacity design values for dynamic amplification for structural cantilever walls are significantly non-conservative. It is also doubtful if the current form of Eq. (2), which has the dynamic amplification factor for shear dependent only on the number of storeys, is capturing the correct causative parameters. The results for both moment and shear force envelopes indicate that dynamic amplification increases as the intensity ratio increases. This would indicate that displacement ductility demand should be included in the design equation, and is in fact obvious from the success of the **MMS** approach in predicting the envelopes. Note that Eq. (6) and (7) can be re-written as:

$$V_i = (V_1^2 + \mu^2 (V_2^2 + V_3^2 + ...)^{0.5} \quad (8)$$

and

$$M_i = (M_1^2 + \mu^2 (M_2^2 + M_3^2 + ...)^{0.5} \quad (9)$$

where the modal shears V_1, V_2, etc, and modal moments M_1, M_2 etc are calculated from the inelastic spectrum in accordance with normal design to NZS4203. The form of Eqs. (8) and (9) indicates that the dynamic amplification should be directly proportional to the displacement ductility demand.

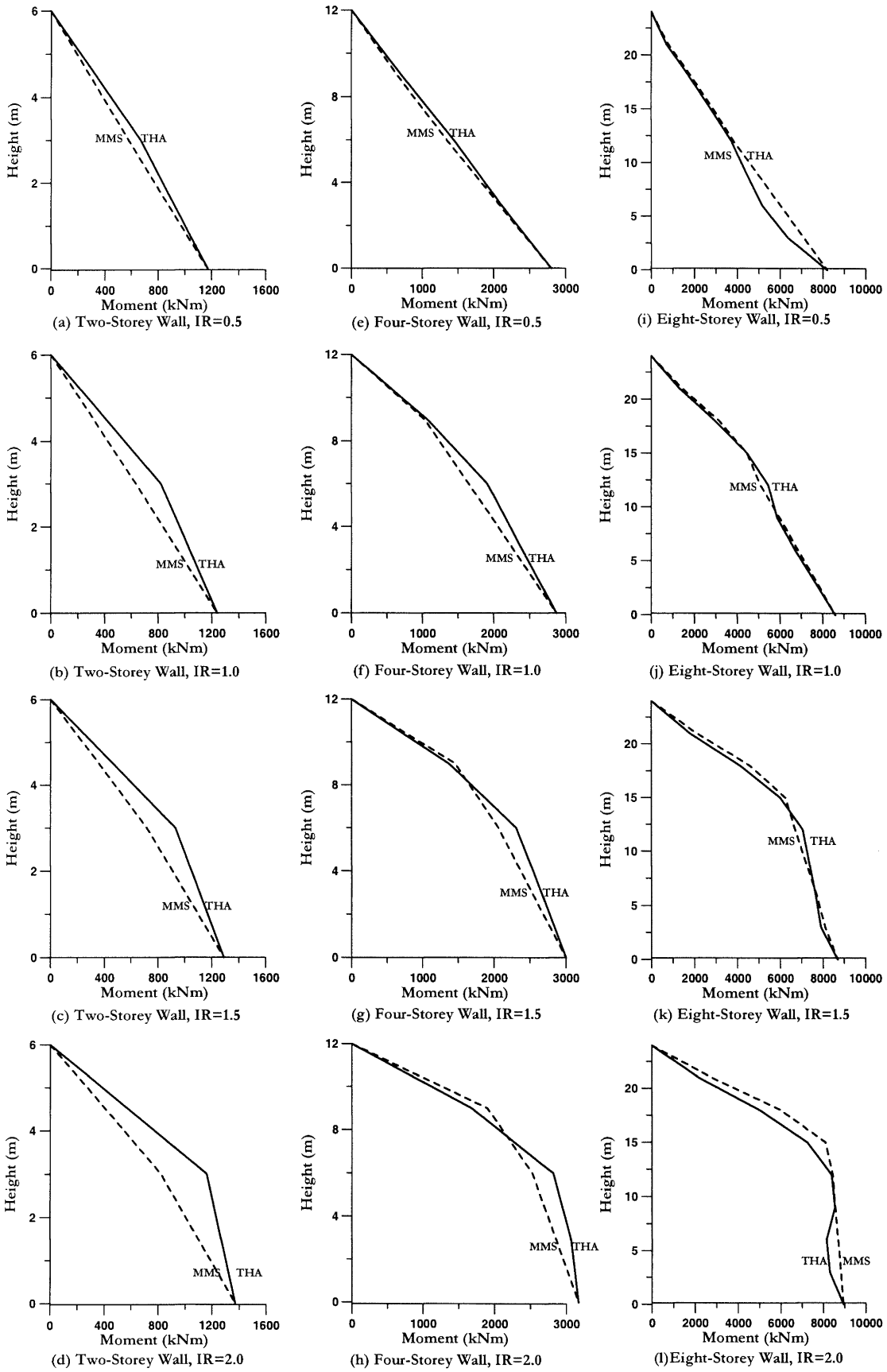

Figure 8. Comparison of Modified Modal Superposition (MMS) Moment Envelopes with Results of Inelastic Time-History Analysis for Different Seismic Intensities.

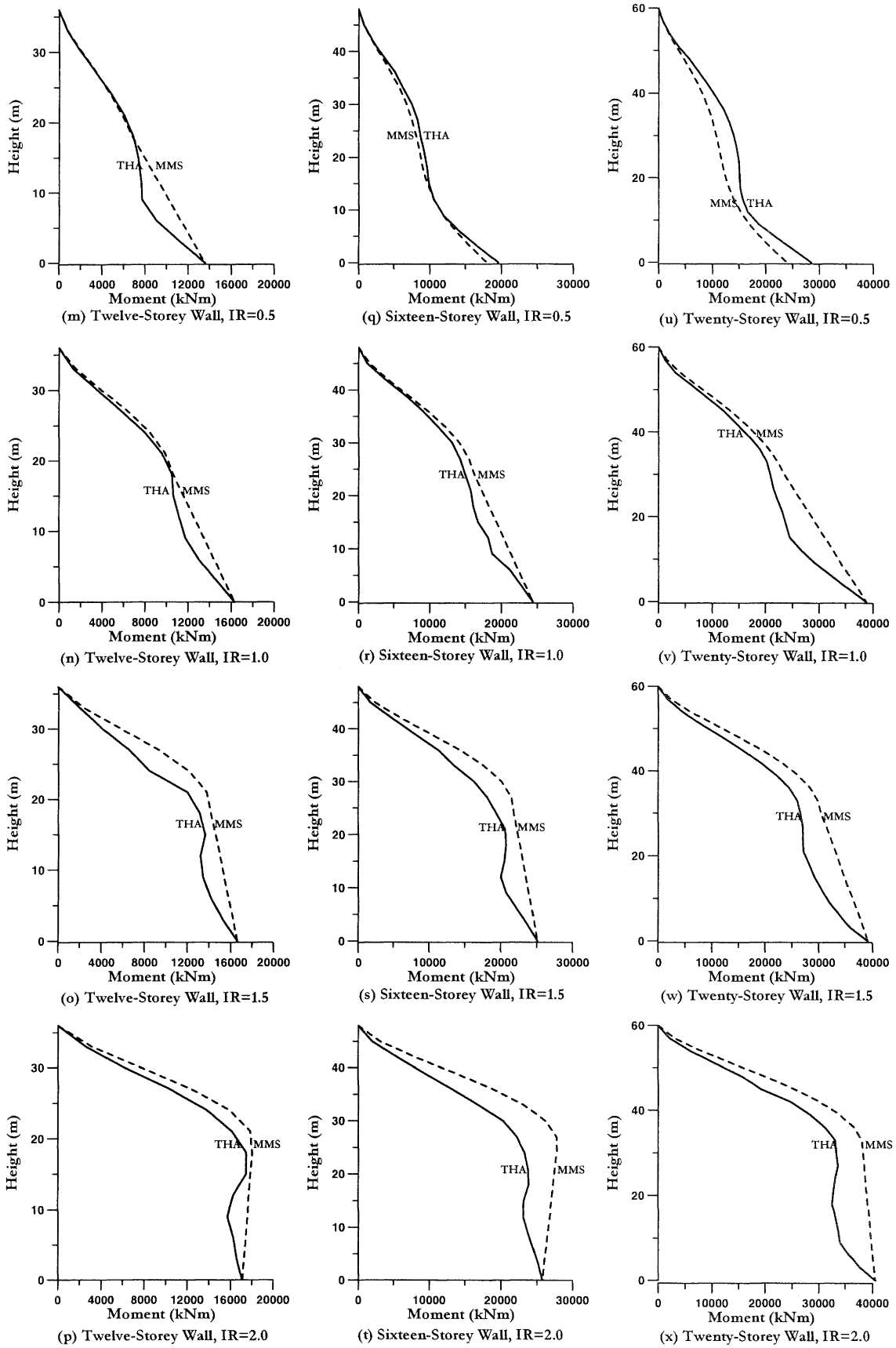

Figure 8. (cont). Comparison of Modified Modal Superposition (MMS) Moment Envelopes with Results from Inelastic Time-History Analysis for Different Seismic Intensities.

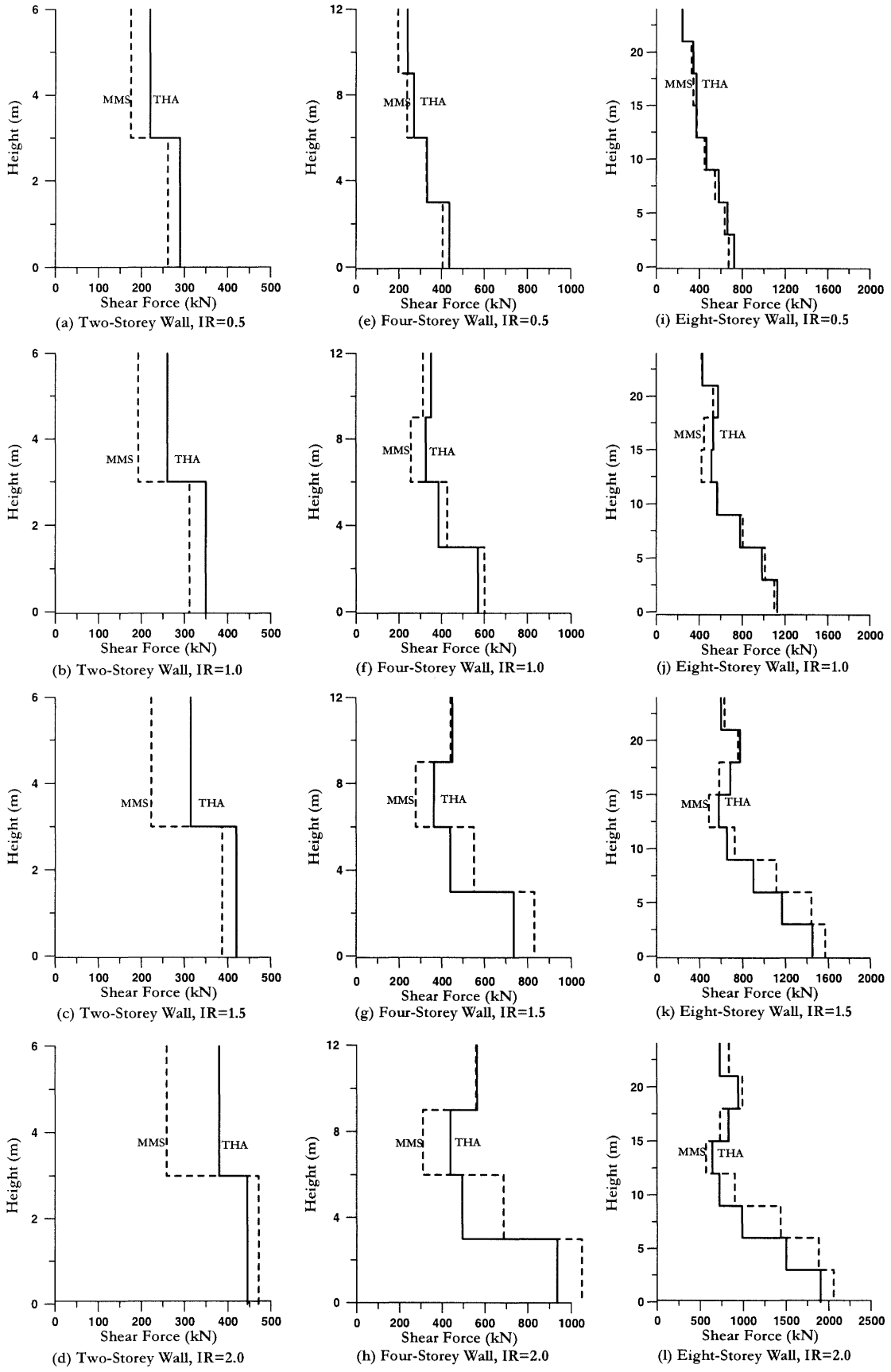

Figure 9. Comparison of Modified Modal Superposition (MMS) Shear Force Envelopes with Results from Time-History Analyses for Different Seismic Intensities.

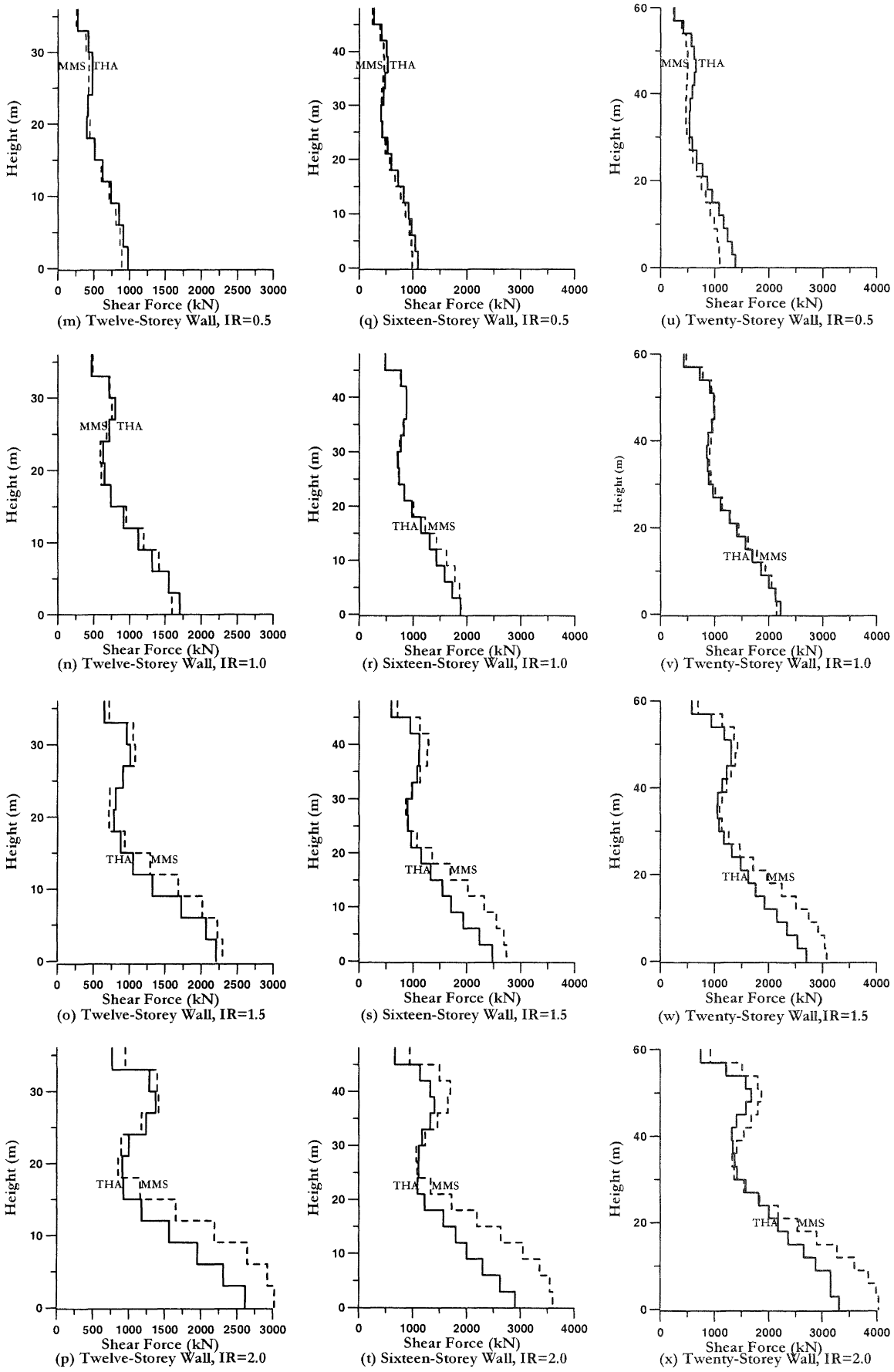

Figure 9. (cont) Comparison of Modified Modal Superposition (MMS) Shear Force Envelopes.

Also, it would appear that the number of storeys should be less significant than the elastic period of the wall. Again this is obvious from consideration of the basis of the **MMS** approach. It is thus of interest to see whether a simple design expression, incorporating both ductility and period can produce realistic estimates of dynamic amplification. Clearly to attempt this for all heights of the buildings would be unrealistic. If such accuracy is desired, then the **MMS** approach should be directly used. However, examination of the shear force profiles indicates that the **DBD** profile shape (which is essentially the same as the **ELF** shape) would provide a conservative envelope to the shear force profile if the base shear was correctly estimated.

Figure 10 plots the relationship between displacement ductility factor, elastic period, and wall base dynamic amplification factor for shear force, ω_v. The average results for the different walls, at different intensity ratios are plotted as data points. It is seen that the relationship between ω_v and μ is indeed effectively linear for any given wall. Also plotted in Figure 10 are the predictions for dynamic amplification based on the expression:

$$\omega_v = 1 + \mu \cdot B_{(T)} \text{ where}$$

$$0.067 \le B_{(T)} = 0.067 + 0.4(T - 0.5) \le 1.15 \quad (10)$$

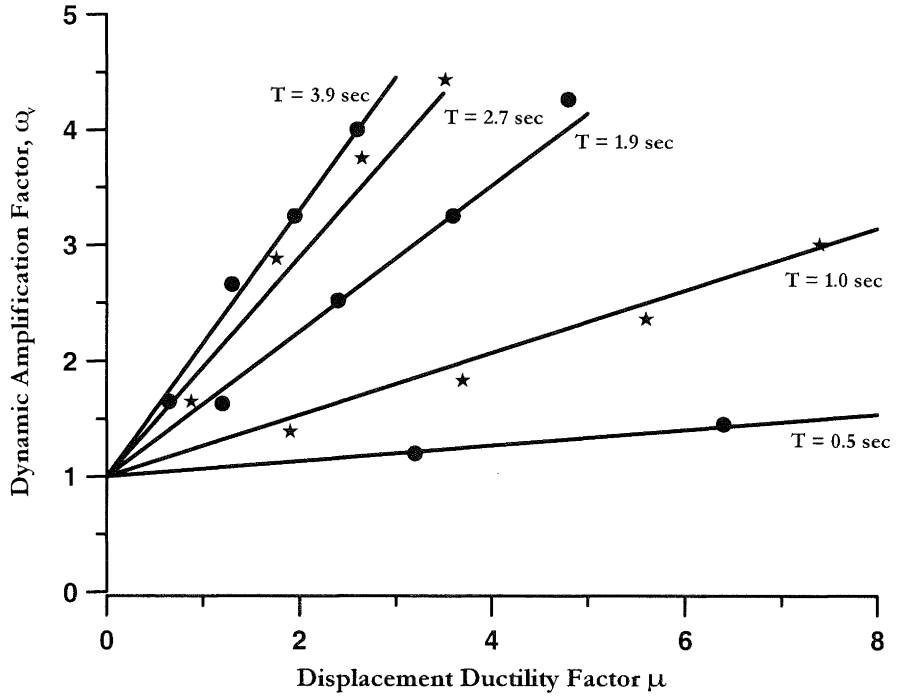

Figure 10. Wall Base Shear Force Dynamic Amplification Related to Period and Ductility(data points from time-history analyses; lines from Eq.(10).

It will be seen that the agreement between Eq. (10) and the averaged time-history results is excellent. Note that significant dynamic amplification is expected even for μ=1.0, for the walls with high elastic periods. This should not be surprising, since the elastic modal shear forces from higher modes exceed those of the first mode for long-period buildings. When flexural overstrength is considered, the base shear force is thus:

$$V_R = \phi^o \omega_v V_E \text{ where } \omega_v = 1 + \frac{\mu}{\phi^o} B_{(T)} \quad (11)$$

with $B_{(T)}$ given in Eq. (10). Note that the effective ductility is reduced by the overstrength factor.

It would clearly also be possible to develop an expression for the moment envelope, dependent on period and ductility. From examination of the profiles of Fig. 8, the obvious form for the envelope would be bilinear, with a change in slope at mid-height of the wall. It would seem, however that a simple choice with the moment at mid-height equal to 0.75 times the wall base moment would be adequately conservative in all cases, at the design intensity.

3. CONCLUSIONS

The analyses presented in this paper indicate that current levels of dynamic amplification for cantilever wall buildings are inadequate to provide dependable capacity protection. Two proposed replacements have been suggested: one based on a modification to modal response spectrum design, and the other in the form of dynamic amplification factors to be applied to base shear from single-mode design methods, such as the NZS4203 **ELF** approach, or direct displacement-based design.

An important consequence of the results is the need to consider the possibility of occurrence of intensities higher than the design level. The results indicate that not only will the ductility demand increase, but so will the shear forces (and to a lesser extent, moment profiles). It would appear philosophically unacceptable for failure to occur in a larger-than-design effect due to failure-mode change resulting from

an increase in the ratio of shear force to moment at intensities above the design level.

Analyses reported elsewhere (Priestley, 2003) indicate that the **MMS** approach, though providing accurate estimates of capacity moment and shear profiles in cantilever walls, is generally unacceptably conservative for frame buildings. It is initially puzzling why the **MMS** approach should work so well for cantilevers but not for frames. It would appear that the answer to this may lie in the effect of ductility on the higher mode characteristics – particularly the periods. A series of analyses on the wall and frame structures considered in these studies was carried out where the stiffnesses for members with plastic hinges were reduced to 0.1 times their initial elastic values, implying member ductility factors of about 10. For the wall structures the second mode period was increased by less than 35%, while for the frame structures the second mode period was increased by at least 125%. It will also be recalled that the ratio of first to second mode periods is approximately 1:5 for cantilever walls, and approximately 1:3 for frames. As a consequence of these two effects, the response of the critical second mode tends to stay on, or rise to, the peak plateau of the acceleration response spectrum for cantilever walls as the wall responds inelastically, and hence the initial elastic response provides a good estimate of the higher mode forces. With frames, the higher mode periods lengthen to the extent that their response slides down the constant velocity slope of the acceleration response spectrum, reducing the higher mode forces as the structure develops ductility.

Note that the behaviour of both walls and frames analysed in these studies support this explanation. For stiff short-period walls, it was found that the **MMS** approach was slightly non-conservative. This would be expected as the higher mode periods lengthen slightly and rise to the constant acceleration plateau (see Fig. 2), increasing higher mode force levels. For the very long period walls, the **MMS** approach was slightly conservative, as higher mode periods exceeded the constant acceleration plateau. Response of a stiff three-storey tube frame, reported in (Priestley, 2003) which was shorter and stiffer than the other frames analysed, was quite well predicted by the **MMS** approach, which gave very conservative representation of the more flexible frames.

The paper also identified two areas, which while not new, should concern New Zealand designers. First, design for the most seismically active regions of New Zealand uses a design acceleration response spectrum that would be considered to be appropriate, in Europe, for a peak ground acceleration of 0.27g, despite New Zealand generally being considered more seismically active than Europe, and capable of generating much larger earthquakes. Second, design to the maximum permitted ductility levels in the Loadings Code will generally result, even for cantilever wall buildings, in drift levels that exceed the code limits.

4. ACKNOWLEDEMENTS

Much of the dynamic analysis reported in this paper was carried out by Alejandro Amaris as part of his MS research project at the European School for Advanced Studies in Reduction of Seismic Risk, Pavia, Italy. His diligent work is gratefully acknowledged.

5. REFERENCES

Blakeley, R.W.G, Cooney, R.C., and Megget, L.M. (1975). Seismic Shear Loading at Flexural Capacity in Cantilever Wall Structures. *Bulletin, New Zealand National Society for Earthquake Engineering,* **8**(4), pp 278-290.

Carr, A.J. (1998). Ruaumoko – A Program for Inelastic Dynamic Analysis. *Dept. of Civil Engineering, University of Canterbury,* Christchurch.

CEN, (1998). Eurocode 8- Design Provisions for Eathquake Resistance of Structures, ENV 1998-2. *Comite Europeen de Normalization*, Brussels.

Eibl, J. and Keintzel, E. (1998). Seismic Shear Forces in RC Cantilever Shear Walls. *Proceedings, 9th World Conference on Earthquake Engineering,* Paper 9-1-1, Tokyo-Kyoto.

IBC, (2000). *International Building Code.* International Code Council, Falls Church, Virginia.

NZS3101, (1995). Concrete Structures Standard. Part 1 – The Design of Concrete Structures, and Part 2- Commentary. *Standards New Zealand,* Wellington.

NZS4203, (1992). Code of Practice for General Structural Design and Design Loadings for Buildings. Vols 1 – Code of Practice – and 2 – Commentary . *Standards New Zealand,* Wellington.

Park,R. and Paulay,T, (1975). Reinforced Concrete Structures, *John Wiley and Sons,* New York.

Priestley, M.J.N. (2000). Performance-Based Seismic Design. *12th World Conference on Earthquake Engineering – Keynote Address,* Auckland. CD-ROM.

Priestley, M.J.N. (2003). Myths and Fallacies in Earthquake Engineering, Revisited. *IUSS Press*, Pavia.

Priestley, M.J.N. and Amaris, A.D. (2002). Dynamic Amplification of Seismic Moments and Shears in Cantilever Walls. *European School for Advanced Studies in Reduction of Seismic Risk.* Research Dept. No.ROSE-2002/01, Pavia.